RSC Advances

COMMUNICATION

View Article Online
View Journal | View Issue

Published on 19 May 2014. Downloaded by Xiamen University on 12/07/2015 10:38:54.

Cite this: *RSC Adv.*, 2014, **4**, 24773

Received 28th March 2014
Accepted 19th May 2014

DOI: 10.1039/c4ra02755h

www.rsc.org/advances

Green interfacial synthesis of two-dimensional poly(2,5-dimethoxyaniline) nanosheets as a promising electrode for high performance electrochemical capacitors†

Changzhou Yuan,*[ac] Longhai Zhang,[a] Linrui Hou,[a] Jingdong Lin*[b] and Gang Pang[a]

2D poly(2,5-dimethoxyaniline) nanosheets were first designed and tailored as intriguing pseudo-capacitive electrode for advanced supercapacitors *via* green interfacial synthetic strategy, and yielded large specific capacitance (SC) and remarkable SC retention at high rates in 1 M HCl electrolyte.

Recently, electrochemical capacitors (ECs) are gaining increasing research interest worldwide because of their attractive ability to deliver larger power density and longer cycling life than common rechargeable batteries and energy density higher by several orders of magnitude than conventional dielectric capacitors.[1] Among the typical electroactive materials for ECs, organic conducting polymers (CPs),[2–4] particularly polyaniline (PANI),[2,4] has captured extensive attention for potential ECs application due to its low cost, ease of synthesis, reversible control of electrical properties by charge transfer doping–dedoping and protonation, and intriguing pseudo-capacitive nature. To further enhance the processability of the PANI for commercial application, numerous efforts have been directed to PANI derivates.[5] However, the substitution of groups in phenyl ring or N-position of PANI units commonly results in the decrease of electronic conductivity,[6] which does not favor the efficient energy storage, particularly at high rates. Fortunately, di-substituted poly(2,5-dimethoxyaniline) (PDMA) with methoxy ($-OCH_3$) groups substituted at *ortho-* and *meta-* positions has shown high electrical conductivity similar to that of the PANI.[5,7–10] Nevertheless, little has been reported about the PDMA for ECs so far. Furthermore, the PDMA samples were generally fabricated *via* chemical oxidative polymerization by using a variety of strong oxidants, *e.g.*, $S_2O_8^{2-}$,[7] Fe^{3+},[9] a $S_2O_8^{2-}/Fe^{3+}$ binary oxidant.[5] Consequently, it is of great significance but still is a great challenge to explore facile yet efficient strategies using greener and milder oxidants for the fine fabrication of high performance nano-structured PDMA for advanced ECs.

Since the development of interfacial polymerization method by Huang for the controllable synthesis of classical PANI nanofibers,[11] elegant interfacial fabrication has been well extended to prepare various CPs and even CP-based composites by the unique liquid–liquid interface of two immiscible liquids consisting of polar and nonpolar solvents.[2,8,12] The inhomogeneous and nanometer-scale interfacial region was endowed with unusual molecular aggregation and orientation, referenced to the bulk solution,[2,8,11–13] favoring the fine construction of nanostructured materials. Unfortunately, some toxic organics (*e.g.*, toluene, chloroform, CCl_4, *etc.*) were usually applied to build a heterogeneous interface.[2,11,13] Therefore, other environmentally-benign and green non-aqueous solvents were urgently required for the efficient interfacial synthesis system.

Based on the above consideration, in this communication, we first developed an efficient water/ionic liquid (IL) green

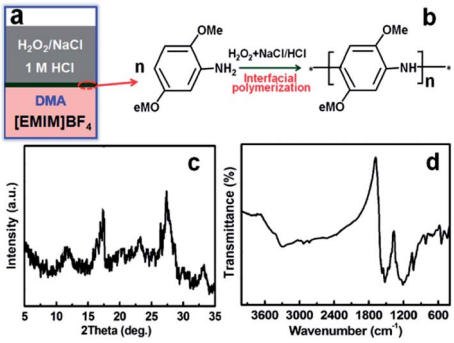

Fig. 1 Schematic illustration for the green interfacial synthesis (a) and polymerization process (b), XRD pattern (c), and FT-IR spectrum (d) of the resulting 2D PDMA NS product.

[a]*School of Materials Science and Engineering, Anhui University of Technology, Ma'anshan, 243002, P. R. China. E-mail: ayuancz@163.com*

[b]*Department of Chemistry, College of Chemistry and Chemical Engineering, Xiamen University, Xiamen, 361005, P. R. China. E-mail: jdlin@xmu.edu.cn*

[c]*Chinese Academy of Science (CAS) Key Laboratory of Materials for Energy Conversion, Hefei, 230026, P. R. China*

† Electronic supplementary information (ESI) available: The detailed synthesis condition, materials and characterizations. See DOI: 10.1039/c4ra02755h

Published on 19 May 2014. Downloaded by Xiamen University on 12/07/2015 10:38:54.

interfacial polymerization strategy (Fig. 1a and b) by using H_2O_2 as an appealing mild oxidant without any extra catalysts.[10] And the hydrophilic IL of 1-ethyl-3-methyl imidazolium tetrafluoroborate ([EMIM]BF_4) was applied to build a prosperous interfacial platform for preparing novel two-dimensional (2D) PDMA nanosheets (NSs) with desirable electronic conductivity and large specific surface area (SSA). The as-obtained PDMA NSs were further utilized as intriguing electroactive materials for ECs. Strikingly, the as-fabricated 2D PDMA NSs delivered large specific capacitance (SC) and long-term electrochemical stability at large current densities in 1 M HCl aqueous electrolyte.

The experimental details are systematically presented in ESI (ESI†). Herein, an efficient green synthetic system, where the unique H_2O/[EMIM]BF_4 interface avoids the use of other poisonous organic solvents, and a much greener H_2O_2 was used as an mild oxidant, was developed for the chemical oxidation polymerization of the PDMA, significantly facilitating its large-scale synthesis. Fig. 1c shows the typical powder X-ray diffraction (XRD) pattern of the as-prepared dark green PDMA product. Five diffraction peaks are evident at $2\theta = 11.5°$, 17°, 24°, 27° and 33°, and can be ascribed to the (001), (011), (100), (110) and (111) planes of the PDMA, respectively.[9] In particular, the former three peaks are due to the presence of dopant anion Cl^- in the PDMA chains.[9] The peak centred at ~27° represents the characteristic distance between the ring planes of benzene rings in adjacent chains or the close contact inter-chain distance, while the another peak at ~33° may be attributed to periodicity, which is perpendicular to the polymer chain.[7] The Fourier transform infrared (FT-IR) spectrum of the resultant PDMA is demonstrated in Fig. 1d. In particular, the peak at 1462 cm^{-1} is originated from asymmetrical bending vibration of $-OCH_3$ groups, and the bands at 1201 and 1025 cm^{-1} correspond to asymmetric and symmetric stretches of the =C–O–C, respectively. The three bands observed here clearly verify the existence of methoxy groups in the final PDMA NSs.[8] When other oxidants, such as, $FeCl_3$ or $(NH_4)_2S_2O_8$ (APS), are further used for the interfacial polymerization both PDMA products are obtained, as evident in the FT-IR spectra (Fig. S1, ESI†), and are denoted as PDMA–$FeCl_3$ and PDMA–APS, respectively.

Fig. 2a–d show the representative field-emission scanning electron microscopy (FESEM) images of the resultant PDMA NS product. Clearly, a large scale of 2D NSs with rippled silk morphology, similar to graphene structure, is demonstrated, indicating the ultrathin nature of the PDMA NSs. It is due to the much larger lateral size than the longitudinal size that the morphology of bending, curling and crumpling is clearly presented. The thickness of the 2D NSs is estimated to be ~20 nm, as shown in Fig. 2d. A large SSA is calculated to be ~175 $m^2\ g^{-1}$ based on the N_2 adsorption-desorption measurement (Fig. S2, ESI†) for the as-obtained PDMA NS sample accordingly, owing to the unique 2D ultrathin feature. As a sharp contrast, some nanoscale granular aggregations are shown for PDMA synthesized *via* ordinary homogeneous synthesis (Fig. S3, ESI†). Particularly, much thicker NSs with a thickness of ~50 nm are observed (Fig. S4, ESI†) when NaCl is absent from the synthetic process. The abnormal phenomenon should be ascribed to the peculiar water/IL interface due to the lower ionic strength of water phase in this case. More interestingly, distinct irregular aggregation morphologies are further presented for the PDMA–$FeCl_3$ and PDMA–APS samples (Fig. S5, ESI†). Consequently, it is easy to conclude that the synergetic effect of the unique non-equilibrium water/IL interface and the appealing oxidant H_2O_2 plays an important role in the controllable synthesis of 2D PDMA NSs. The inherent formation mechanism of such unique 2D PDMA still requires further study, which is currently undergoing.

To evaluate the electrochemical capacitive performance of the resultant PDMA NSs, cyclic voltammetry (CV) and chronopotentiometry (CP) were subsequently carried out in 1 M HCl aqueous electrolyte at room temperature (RT). Fig. 3a shows the typical *I–E* response of the 2D PDMA NS electrode at a CV sweep rate of 2 mV s^{-1}. A pair of redox peaks within −0.2 to 0.3 V

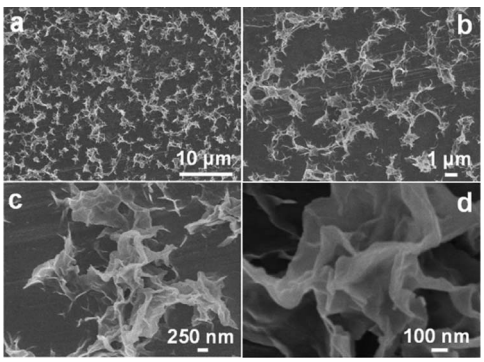

Fig. 2 FESEM (a–d) images of the as-obtained PDMA NSs.

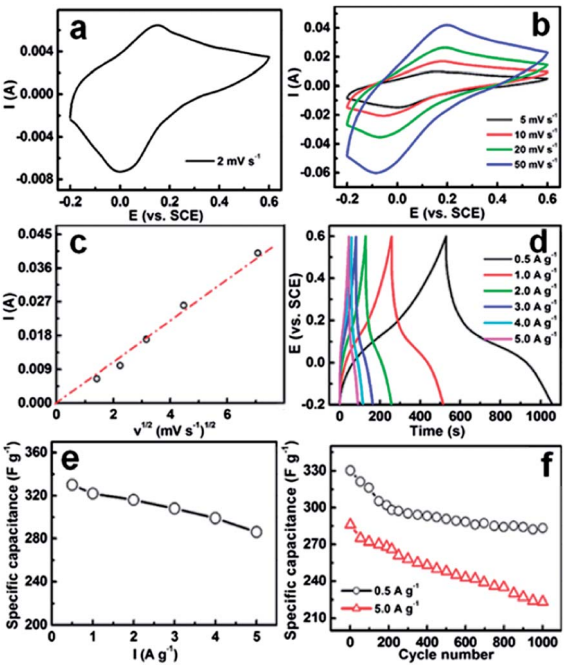

Fig. 3 CV curves (a and b), *I vs.* $v^{1/2}$ (c), CP plots (d), SC as a function of current density (e), and cycling performance (f) of the as-synthesized 2D PDMA NSs.

This journal is © The Royal Society of Chemistry 2014

Published on 19 May 2014. Downloaded by Xiamen University on 12/07/2015 10:38:54.

(*vs.* SCE) are obviously visible, and reveal that the typical pseudo-capacitive nature is mainly governed by inherent Faradaic redox reactions occurring on and/or near the surface of the 2D NSs. Impressively, the electrochemical response currents subsequently increase while the CV shape almost remains the same with the increase of the scan rates, as demonstrated in the multi-scan rate voltammograms (Fig. 3b), suggesting good electrochemical capacitance of the unique PDMA NS electrode over the entire range of scan rates from 2 to 50 mV s^{-1}. Fig. 3c depicts the oxidation peak current of the as-prepared PDMA NSs as a function of the square root of scan rate ($v^{1/2}$). The linear relationship of I *vs.* $v^{1/2}$ shows a unique diffusion-control process.[14] The appealing conductivity (~0.07 S cm^{-1}) of the PDMA NSs may facilitate the rapid electron transfer rate, and thus the NS electrode process is a diffusion controlled process rather than a kinetic controlled one.[14] In addition, galvanostatic CP test was then performed to estimate the SC of the PDMA NSs at a series of current densities ranged from 0.5 to 5 A g^{-1} in a potential window of −0.2 to 0.6 V (*vs.* SCE). The nonlinear CP plots with symmetric shape demonstrate striking pseudo-capacitive characteristics, as displayed in the CP curves of Fig. 3d. It is worth noting that the high coulombic efficiency of >99% is delivered over all the current densities ranging from 0.5 to 5 A g^{-1}, as seen in Fig. 3d, revealing the desirable electrochemical reversibility of the PDMA NS electrode. The charge–discharge measurement is carried out in three consecutive cycles for each current density, and the SC is finally calculated as a mean value of the former three cycles. Fig. 3e presents the SCs corresponding to different current densities in 1 M HCl aqueous solution. The SC of PDMA NSs is calculated as ~330 F g^{-1}, that is, an area specific SC of ~1.9 F m^2 considering its SSA, at a current density of 0.5 A g^{-1}, higher than that of the nanoscale PDMA electrode,[9] and even comparable to other CPs,[2,3,15] and 2D metal oxides,[16] sulphides[17] and selenides NSs.[18] Although the SC decrease of the PDMA NSs is observed with the increase of current density, a SC of ~286 F g^{-1} (*i.e.*, ~1.6 F m^2) can still be achieved even at a high current density of 5 A g^{-1}, which remains approximately 87% of the highest SC value at 0.5 A g^{-1}. This further confirms the excellent high-rate performance of the PDMA NS electrode, which is of significant importance to its practical applications. Particularly, the SCs delivered by the PDMA NS electrode are also much larger than those for PDMA–$FeCl_3$ (~221 F g^{-1} at 0.5 A g^{-1}) and PDMA–APS (~195 F g^{-1} at 0.5 A g^{-1}) samples (Fig. S6, ESI†), which should be ascribed to smaller SSA for the PDMA–$FeCl_3$ (~101 m^2 g^{-1}) and PDMA–APS (~87 m^2 g^{-1}) products. In addition to this, another important factor is that the modest electronic conductivities of the other two must also not be ignored. The conductivities of the PDMA–$FeCl_3$ and PDMA–APS products can be estimated as ~2×10^{-3} and ~6×10^{-3} S cm^{-1} *via* the standard four-probe DC technique on pressed pellets from powder, respectively, which can be further supported by the different intersections of the electrochemical impedance spectroscopy (EIS) plots at the *X*-axis for the three PDMA electrodes (Fig. S7, ESI†). Finally, the PDMA NS electrode demonstrates even smaller charge-transfer resistance of ~0.4 ohm than the PDMA–$FeCl_3$ (~0.9 ohm) and PDMA–APS (~1.3 ohm) electrodes, estimated from the semicircle diameter observed at the high-medium frequency region (Fig. S7, ESI†), which should also be responsible for the large SCs of the unique 2D PDMA NS electrode, particularly at high rates.

The long-term cycling stability is additionally a critical requirement for practical application of ECs. Fig. 3f depicts the SC variation as a function of the cycle number at current densities of 0.5 and 5 A g^{-1} for up to 1000 cycles. It can be observed that the SCs of the PDMA NS electrode gradually reduce, whereas the SC degradations of ~13% and ~22% are observed at 0.5 and 5 A g^{-1}, respectively, continuously over 1000 cycles, indicating its stable long-term cycling performance even at large current density. In contrast, the SC retentions of the two PDMA–$FeCl_3$ and PDMA–APS electrodes (Fig. S8, ESI†) are found as ~18% and ~23%, respectively, after 1000 continuous cycles at a current density of 0.5 A g^{-1}. The abovementioned electrochemical data mentioned strongly highlights the remarkable merits of the PDMA NSs as an advanced electrode to meet the requirements of both long cycling lifetime and large SCs at high rates, which should be attributed to the better electronic conductivity and smaller charge-transfer resistance of the 2D PDMA NSs with rich electroactive sites.

Furthermore, a quasi-supercapacitor is fabricated by two PDMA NS electrodes face to face in 1 M HCl aqueous solution. The electrochemical performance of the PDMA NS-based symmetric supercapacitor is estimated and the typical data was collected (Fig. S9, ESI†). As seen from these typical CV curves (Fig. S9a, ESI†), the current subsequently increases as the scan rate increases, while the CV shape slightly changes, and rapid current response on voltage reversal occurs at each end potential, suggesting its appealing electrochemical capacitance. In addition, based on the CP plots (Fig. S9b, ESI†), the SCs of the symmetric capacitor can be calculated as 78, 75 and 73 F g^{-1} at the current densities of 0.2, 0.5 and 1.0 A g^{-1}, respectively. The specific energy density (E) and power density (P) of the PDMA NS-based symmetric capacitor are impressively calculated as ~3.7 W kg^{-1} and ~304.1 W kg^{-1} at a current density of 1.0 A g^{-1}.

In summary, we have successfully developed an attractive green interfacial strategy to synthesize 2D PDMA NSs, and further applied it as a high performance pseudo-capacitive electrode for ECs. Benefiting from the intriguing 2D NS feature, high electronic conductivity and modest charge-transfer resistance, the as-fabricated PDMA NS electrode delivered large SCs, and stabilized cycling performance coupled with a high coulombic efficiency in 1 M HCl aqueous solution. More significantly, an efficient green avenue is now open for the future development of other low-cost electroactive materials for next-generation ECs.

Acknowledgements

This work was supported by the National Natural Science Foundation of China (no. 51202004), the Natural Science Foundation of Anhui Province (KJ2013A051), and the Opening Project of CAS Key Laboratory of Materials for Energy Conversion (no. 2014001).

Published on 19 May 2014. Downloaded by Xiamen University on 12/07/2015 10:38:54.

Notes and references

1 C. Liu, F. Li, L. P. Ma and H. M. Cheng, *Adv. Mater.*, 2010, **22**, E28; C. Z. Yuan, H. B. Wu, Y. Xie and X. W. Lou, *Angew. Chem., Int. Ed.*, 2014, **53**, 1488; P. Simon and Y. Gogotsi, *Nat. Mater.*, 2008, **7**, 845; B. E. Conway, *Electrochemical Supercapacitors: Scientific Fundamentals and Technological Applications*, Kluwer Academic/Plenum Publishers, New York, 1999.

2 C. Z. Yuan, L. R. Hou, L. F. Shen and X. G. Zhang, *J. Electrochem. Soc.*, 2012, **159**, A1323.

3 L. R. Hou, C. Z. Yuan, D. K. Li, L. Yang, L. F. Shen, F. Zhang and X. G. Zhang, *Electrochim. Acta*, 2011, **56**, 6049; X. J. Lu, H. Dou, C. Z. Yuan, S. D. Yang, L. Hao, F. Zhang, L. F. Shen, L. J. Zhang and X. G. Zhang, *J. Power Sources*, 2012, **197**, 319.

4 Q. Wang, J. Yan, Z. J. Fan, T. Wei, M. L. Zhang and Y. Y. Jing, *J. Power Sources*, 2014, **247**, 197; C. Z. Yuan, L. F. Shen, X. J. Lu and X. G. Zhang, *Chem. Lett.*, 2010, **39**, 850.

5 S. E. Mavundla, G. F. Malgas, P. Baker and E. I. Iwuoha, *Electroanalysis*, 2008, **20**, 2347.

6 R. D. Calleja, E. S. Matveeva and V. P. Parkhutik, *J. Non-Cryst. Solids*, 1995, **180**, 260; A. J. Epstein and A. G. MacDiarmid, *Macromol. Symp.*, 1991, **51**, 217.

7 L. M. Huang, T. C. Wen and A. Gopalan, *Mater. Lett.*, 2003, **57**, 1765; G. D. Storrier, S. B. Colbran and D. B. Hibbert, *Synth. Met.*, 1994, **62**, 179; G. D. Aprano, M. Leclerc, G. Zptti and G. Schiavon, *Chem. Mater.*, 1995, **7**, 33.

8 A. Muslim, T. Abdryim and S. Zhi, *Polym. Sci.*, 2011, **53**, 480.

9 S. P. Palaniappan, S. R. P. Gnanakan, Y. S. Lee and P. Manisamkar, *Ionics*, 2011, **17**, 603.

10 S. Jain, S. P. Surwade, S. R. Agnihotra, V. Dua, P. A. Eliason, G. J. Morose and S. K. Manohar, *Green Chem.*, 2010, **12**, 585.

11 J. X. Huang, S. Virji, B. H. Weiller and R. B. Kaner, *J. Am. Chem. Soc.*, 2003, **125**, 314.

12 J. H. Zhu, M. J. Chen, H. L. Qu, X. Zhang, H. G. Wei, Z. P. Luo, H. A. Colorado, S. Y. Wei and Z. H. Guo, *Polymer*, 2012, **53**, 5953; J. G. Wang, Y. Yang, Z. H. Huang and F. Y. Kang, *J. Power Sources*, 2012, **204**, 236; H. Y. Ma, Y. Q. Luo, S. X. Yang, Y. W. Li, F. Cao and J. Gong, *J. Phys. Chem. C*, 2011, **115**, 12048.

13 L. R. Hou, Q. Zhang, L. T. Ling, C. X. Li and S. Chen, *J. Am. Chem. Soc.*, 2013, **135**, 10618; S. Y. Yang, C. F. Wang and S. Chen, *J. Am. Chem. Soc.*, 2011, **133**, 8412; L. R. Hou, L. Lian, L. H. Zhang, T. Wu and C. Z. Yuan, *RSC Adv.*, 2014, **4**, 2374; C. Z. Yuan, L. R. Hou, L. Yang, D. K. Li, L. F. Shen, F. Zhang and X. G. Zhang, *J. Mater. Chem.*, 2011, **21**, 16305.

14 Y. G. Wang, Z. S. Hong, M. D. Wei and Y. Y. Xia, *Adv. Funct. Mater.*, 2012, **22**, 5185; Y. Wang, C. X. Guo, J. H. Liu, T. Chen, H. B. Yang and C. M. Li, *Dalton Trans.*, 2011, **40**, 6388.

15 M. J. Bleda-Martínez, C. Peng, S. G. Zhang, G. Z. Chen, E. Morallón and D. Cazorla-Amorós, *J. Electrochem. Soc.*, 2008, **155**, A672; D. W. Wang, F. Li, J. P. Zhao, W. C. Ren, Z. G. Chen, J. Tam, Z. S. Wu, L. Gentle, G. Q. Lu and H. M. Cheng, *ACS Nano*, 2009, **3**, 1745.

16 C. Z. Yuan, L. Yang, L. R. Hou, L. F. Shen, X. G. Zhang and X. W. Lou, *Energy Environ. Sci.*, 2012, **5**, 7883.

17 C. L. Zhang, H. H. Yin, M. Han, Z. H. Dao, H. Pang, Y. L. Zheng, Y. Q. Lan, J. C. Bao and J. M. Zhu, *ACS Nano*, 2014, **8**, 3761.

18 J. Feng, X. Sun, C. Xu, C. Lin, S. Hu, J. Yang and Y. Xie, *J. Am. Chem. Soc.*, 2011, **133**, 17832.

 This journal is © The Royal Society of Chemistry 2014